Journal of the Korean Association for Shell and Spatial Structures
Vol. 3, No. 2 (통권 8호), pp. 91~99, June. 2003

접합부 특성을 고려한 볼 접합 단층 래티스 돔의 탄소성 좌굴해석

The Elasto - Plastic Buckling Analysis of Ball - Jointed Single Layer Latticed Domes considering the Characteristics of a Connector

한 상 을 Han, Sang-Eul*
권 현 재 Kwon, Hyun-Jae**
김 종 범 Kim, Jong-Bum***

Abstract

The purpose of this study is to analyze the characteristics of the connector having an influence on the elasto-plastic buckling load of ball-jointed single layer latticed domes. As an analytic model, domes are composed of tubular member elements, balls and connectors. The joint system of members in single layer latticed domes has influence on the buckling load. Therefore, in this paper, the variation of the elasto-plastic buckling load by effects of the connectors characteristics is analyzed. The structural behavior of the connector is investigated by following points; (1) the length of rigid zone, (2) looseness of screw and (3) the diameter of connector. In addition, the elasto-plastic buckling analysis is carried out through the variation of the connectors section of yielding part, and then the buckling mode of the dome is examined. As a result, it is emphasized that the characteristics of the connector have significant effects on the buckling load of latticed domes.

keywords : ball-joint, elasto-plastic buckling load, connector, single layer latticed dome

1. Introduction

The material and geometrical non-linearity should be considered simultaneously for the exact elasto-plastic buckling analysis of single layer latticed domes. Thus, both ends and the central part of the tubular member elements are assumed to be connected by five elasto-plastic springs which was proposed by Kato[1] to find out the yielding part of the member. Generally, the node is assumed to be a pin or rigid joint for the simplification of analysis. But the Mero system that is used mostly for the spatial structures has intermediate properties between a pin and rigid joint. Several studies based on the property of this semi-rigid joint were as Experiment and elasto-plastic buckling analysis of ball-jointed single layer reticulated domes by Suzuki[2], Elasto-plastic buckling loads of latticed shells with elastic springs at both ends of members by Kato and Loading test and elasto- plastic buckling analysis of a single layer latticed dome by Ueki[3] and so on.

Based on the results of previous studies, it is shown analytically that the buckling load of the ball-jointed system is low when compared with that of the rigid joint system. And it is known that present results are caused by the property of the connector. Therefore, in this paper, we performed the numerical analysis to investigate the structural characteristics through the some models similar to the practical ball-jointed single layer latticed dome and evaluated the variation of elasto-plastic buckling load of domes by change of connectors

* 정회원, 인하대학교 건축학부 교수
** 삼우구조기술사무소 대리
*** 학생회원, 인하대학교 건축학부 박사과정

stiffness also.

2. Modeling of the Unit Member And Joint

<Fig. 1> shows the model proposed by Kato for the unit member of ball-jointed single layer latticed domes. Each member is composed of two elastic beam elements and five elasto-plasic springs. Stiffness matrix of elastic elements is derived from the slope deflection method and then a stiffness matrix of unit member can be obtained by assembling stiffness matrix of the each element.

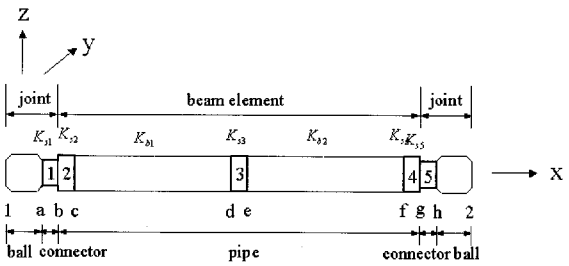

〈Fig.1〉 Modeling of the unit member

Joint (ball + connector) :
rigid zone (1-a) + elasto-plastic spring [1](a-b)
..... $[r_1]^T[k_{s1}][r_1]$

Beam element (pipe) :
elasto-plastic spring [2](b-c) ..... $[k_{s2}]$
+ elastic element (c-d) ..... $[k_{b1}]$
+ elasto-plastic spring [3](d-e) ..... $[k_{s3}]$
+ elastic element (e-f) ..... $[k_{b2}]$
+ elasto-plastic spring [4](f-g) ..... $[k_{s4}]$

Joint (connector + ball) :
elasto-plastic spring [5](g-h) + rigid zone (h-2)
..... $[r_2]^T[k_{s5}][r_2]$

The stiffness matrix of unit member can be derived as following Eq (1) by principle of total potential energy.

$$\delta U_{s1} + \delta U_b + \delta U_{s2} - \delta E =$$

$$\delta\{d_1^T\ d_b^T\ d_c^T\ d_d^T\ d_e^T\ d_f^T\ d_g^T\ d_2^T\}$$

$$\begin{bmatrix} [r_1]^T[k_{s1}][r_1]^T & & & & & & & \\ & [k_{s2}] & & & & & & \\ & & [k_{b1}] & & & & & \\ & & & [k_{s3}] & & & & \\ & & & & [k_{b2}] & & & \\ & & & & & [k_{s4}] & & \\ & & & & & & [r_1]^T[k_{s1}][r_1]^T & \end{bmatrix} \begin{Bmatrix} d_1 \\ d_b \\ d_c \\ d_d \\ d_e \\ d_f \\ d_g \\ d_2 \end{Bmatrix}$$

$$- \delta\{d_1^T\ d_2^T\}\begin{Bmatrix} f_1 \\ f_2 \end{Bmatrix} = 0 \qquad (1)$$

Where, d_i is displacement of i node. And Eq.(1) can be simplified as following.

$$\delta\{d_{12}^T\ d_{bg}^T\}\begin{bmatrix} A & B \\ B^T & C \end{bmatrix}\begin{Bmatrix} d_{12} \\ d_{bg} \end{Bmatrix}$$

$$-\delta\{d_{12}^T\ d_{bg}^T\}\begin{Bmatrix} f_{12} \\ 0 \end{Bmatrix} = 0 \qquad (2)$$

Eq.(2) is expressed as following.

$$[[A] - [B][C]^{-1}[B]^T]\{d_{12}\} = \{f_{12}\} \quad (3)$$

Where, $[[A] - [B][C]^{-1}[B]^T]$ is the stiffness matrix of unit member, $[k]$.

It is considered that springs resisting axial deformation of x-axis, and rotation of y and z-axis are regularized with the elastic spring before yielding and with the plastic spring after yielding by axial force and bending moment. Plastic springs are assumed to flow yielding surface shown in <Fig. 2>. The yielding criterion can be expressed as

$$f = (N/N_p)^2 + \sqrt{(M_y/M_p)^2 + (M_z/M_p)^2} - 1$$
$$= N^2 + M - 1 \qquad (4)$$

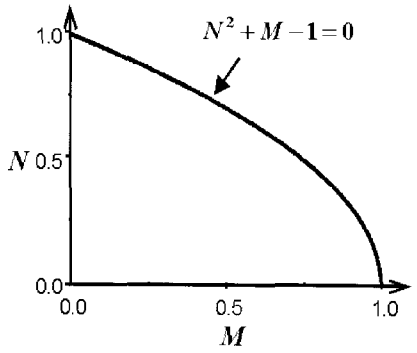

〈Fig. 2〉 Yielding surface

Where, N and N_p are axial force and axial force of yielding. M_y and M_z are y, z-axis rotational elastic moment of spring and M_p is plastic moment of element. If the value of f_y is less than 1, it means elastic state and in case of more than 1, it means plastic state.

The practical end part of the element connected by spherical ball as a connector is modeled as shown in <Fig. 3> Where, D_c and D_s represent diameters of connector and steel pipe, and λ_1 and λ_2 represent ratio of rigid zone and effect on the looseness of screw respectively. That is, $\lambda_1 l_0$ means length of rigid zone and $\lambda_2 l_0$ means length of connector. Also, effect on the looseness of screw is supposed to be changed according to λ_2.

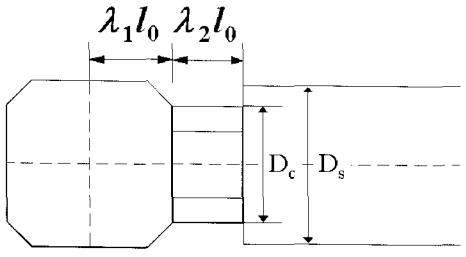

〈Fig. 3〉 Modeling of the joint

The equation of the rotational rigidity of the semi-rigid connector (K_B) at both ends of members can be written as.

$$\chi = K_B \cdot \frac{l_o}{EI_y} \left(= K_B \cdot \frac{l_o}{EI_z} \right) \tag{5}$$

Where, the parameter χ is represents the ratio of the rotational spring rigidity to member bending rigidity. Therefore the rotational rigidity for the connector (K_B) can be expressed by the value of χ in which EI_y and EI_z are y-axis and z-axis member rotational rigidity respectively assumed to be identical in value, and l_0 is member length. If the value of χ is larger than 100, it indicate rigid joint and when that is near to 0, it means pin joint in this paper.

The second moment of inertia and section area of unit member, which are comprised of ball, connector and pipe, can be substituted with equi valent effective second moment of inertia (I_e) and section area (A_e) as follows;

$$I_e = \frac{I_s}{(1-2\lambda_1-2\lambda_2)+2\lambda_2 I_s/I_c} \tag{6}$$

$$A_e = \frac{A_s}{(1-2\lambda_1-2\lambda_2)+2\lambda_2 A_s/A_c} \tag{7}$$

Where, the parameters I_s and I_c are the second moment of inertia of pipe and connector and the parameters A_s and A_c are the section area of pipe and connector respectively.

3. An Analytycal Method and Models

We used load incremental technique based on the Newton Raphson method as the nonlinear numerical algorithm in this paper, which applied (<Fig. 4>) repeatedly the following equation.

$$[{}_tK]\{\Delta D\} = \{P\} - \{F\} \tag{8}$$

Where, $\{P\} - \{F\}$ means the out-of balance force, For the first step of $n+1$,

$$[K(N=N_n)]\{\Delta D_{n+1}^{(1)}\}=\{\Delta P_{n+1}\}-\{F(N=N_n)\} \quad (9)$$

$$\Delta D_{n+1}^{(1)} \rightarrow \Delta N_{n+1}^{(1)} \rightarrow N_{n+1}^{(1)}=N_n+\Delta N_{n+1}^{(1)} \quad (10)$$

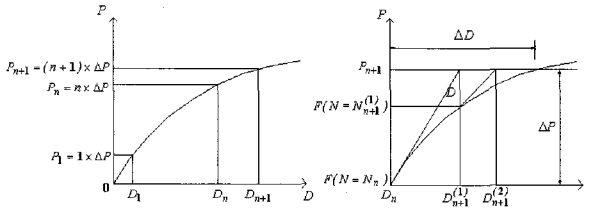

〈Fig. 4〉 Numerical method

For the second step of $n+1$,

$$[K(N=N_{n+1}^{(1)})]\{\Delta D_{n+1}^{(2)}\}=\{\Delta P_{n+1}\} -\{F(N=N_{n+1}^{(1)})\} \quad (11)$$

$$\Delta D_{n+1}^{(2)} \rightarrow \Delta N_{n+1}^{(2)} \rightarrow N_{n+1}^{(2)}=N_{n+1}^{(1)}+\Delta N_{n+1}^{(2)} \quad (12)$$

Judgment condition[5] of convergence about out-of-balance force follows Eq. (13), and tolerance is assumed to be 0.01.

$$||g||-(g^Tg)^{1/2}< \beta||P_e|| \quad (13)$$

Where, g is out-of-balance force vector, P_e is the current total external load vector, and β is tolerance. And flowchart shown in <Fig. 5> is used for the numerical analysis in this paper.

The structural behavior of the dome with two types of boundary condition is investigated such as pin and roller supported grid domes as shown in <Fig. 6>. Member properties and dimensions of domes are shown in <Table 1>. The uniform load is applied vertically at each of joints. Values of the parameter λ_1 indicated by <Fig. 3> are increased from 0.01 to 0.04 by 0.01. In addition, the variation of the elasto-plastic buckling load is also investigated based on the values of the parameter λ_2,

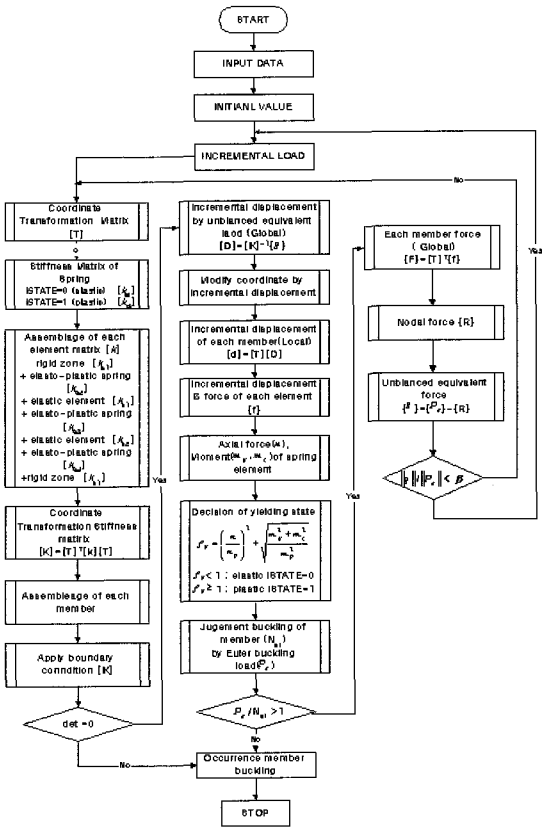

〈Fig. 5〉 Numerical analysis algorithm

having effects on the looseness of screw. The values of the parameter λ_2 are given by 0.01, 0.015, 0.02, 0.25 and 0.03, 4 values of 30mm, 35mm, 40mm and 45mm are used as the diameter of the connector.

〈Table 1〉 Member Properties

<table>
<tr><td colspan="4">Youngs modulus $E(t/cm^2)$
Modulus of strain hardening $E_t(t/cm^2)$
Yield stress $\sigma_y(t/cm^2)$
Member length $l_0(cm)$</td><td colspan="3">2100
21
2.4
300</td></tr>
<tr><td rowspan="2">Pipe</td><td colspan="3">Diameter $D_s(mm)$</td><td colspan="3">Φ139.8×4.0</td></tr>
<tr><td colspan="3">Section area $A_s(cm^2)$</td><td colspan="3">17.07</td></tr>
<tr><td rowspan="4">Connector</td><td rowspan="4">Section area $A_c(cm^2)$</td><td rowspan="4">Diameter $D_c(mm)$</td><td>Φ30</td><td colspan="3">7.07</td></tr>
<tr><td>Φ35</td><td colspan="3">9.62</td></tr>
<tr><td>Φ40</td><td colspan="3">12.56</td></tr>
<tr><td>Φ45</td><td colspan="3">15.90</td></tr>
<tr><td rowspan="2">$L(m)$</td><td rowspan="2">$\theta(^\circ)$</td><td>2°</td><td>23.69</td><td rowspan="2">$H(m)$</td><td rowspan="2">$\theta(^\circ)$</td><td>2°</td><td>1.66</td></tr>
<tr><td>3°</td><td>23.30</td><td>3°</td><td>2.47</td></tr>
</table>

4. Variation of the Elasto-Plastic Buckling Load According to Characteristics of a Connector

For this model shown in <Fig 6>, we investigated the variation of elasto-plastic buckling load for three variables - the length of rigid zone ($\lambda_1 l_0$), the looseness of screw ($\lambda_2 l_0$) and the connectors diameter.

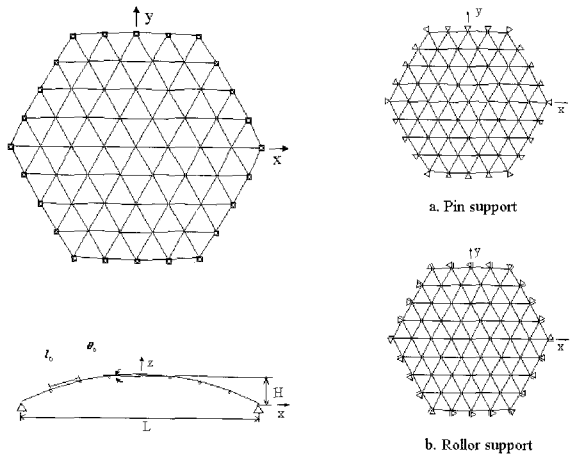

〈Fig. 6〉 Dome geometry

<Fig. 7> shows the variation of the elasto-plastic buckling load according to the length of rigid zone ($\lambda_1 l_0$), where the diameter of the connector and parameter λ_2 are 35mm and 0.01 respectively and P_{cr}^{pl} is the elasto-plastic buckling load determined by analysis. Fig. 7 indicates that the length of rigid zone has not much effect on the elsto-plastic buckling load for the both pin and roller cases except that P_{cr}^{pl} increase as the length of rigid zone at $\varkappa = 100$, $\theta = 3^\circ$ with pin support.

<Fig. 8> shows the variation of the elasto-plastic buckling load according to the looseness of screw ($\lambda_2 l_0$) with connectors diameter of 35mm and pa rameter λ_1 of 0.03. When the value of λ_2 is less than 0.02 Fig. 8 shows that the reduction rate of elasto-plastic buckling load is very large. Therefore, it is recognized that the initial instability be-

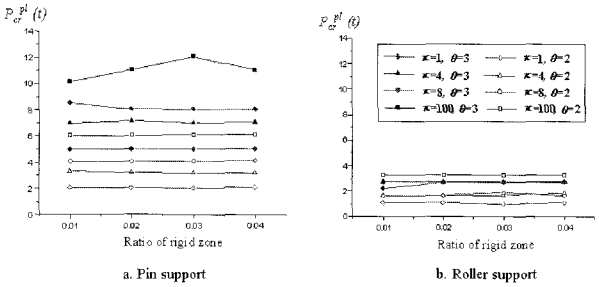

〈Fig. 7〉 The relation of buckling load vs. rigid zone

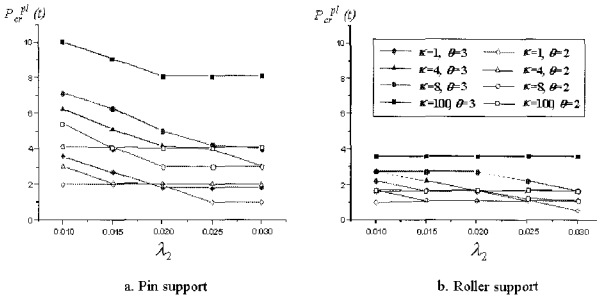

〈Fig. 8〉 The relation of buckling load vs. loosness of screw

comes an important factor when screw begins to loose.

<Fig. 9> shows the variation of P_{cr}^{pl} as the connectors diameter is increased with 30, 45, 40 and 45mm with parameters λ_1 and λ_2 of 0.03 and 0.01 respectively. As shown in <Fig. 9>, for the pin support case, is increased, if connectors diameter becomes to be large in size. The elasto-plastic buckling load increased rapidly in case of rather than. For the roller support case, P_{cr}^{pl} is increased slightly as the connectors diameter becomes to be large in size. The elasto-plastic buckling load increased rapidly in case of $\theta = 3^\circ$ rather than $\theta = 2^\circ$. For the roller support case, P_{cr}^{pl} is increased slightly as the connectors diameter becomes to be large in size. However, in this case, the connectors diameter has not much effect on the elasto-plastic buckling load.

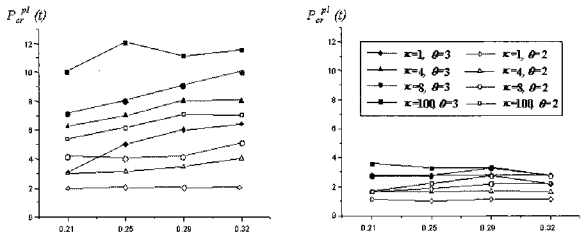

〈Fig. 9〉 The relation of buckling load vs. diameter of connector

5. Elasto-Plastic Analysis with Variation of the Yielding Section

The overall buckling is mostly occurred after yielding of the connectors in ball-jointed single layer latticed domes. Therefore, the buckling load can be increased by raising strength of the yielding parts of connector. In this paper, the numerical analysis with variation of the connectors yielding part is performed and then the buckling mode of the dome is examined. The analytical models are three types of geometric forms as shown in <Fig. 10> Grid and Lamella Network Domes are all symmetric, but the Geodesic Dome is asymmetric.

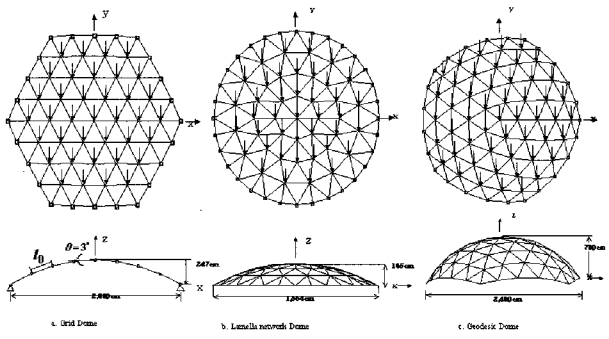

〈Fig. 10〉 Geometirc Formes

The length of each member is different except the Grid Dome. Each single layered dome is analyzed by these three cases.

1. Connector and pipe with all the same section area -Pipe $\Phi-139.8\times4.0$, connector- $\Phi-35$
2. Case increasing the connectors section of yielding part -Pipe $\Phi-139.8\times4.0$, connector- $\Phi-40$
3. Case increasing the pipes section of yielding part. -Pipe $\Phi-165.2\times4.5$, connector- $\Phi-40$

Also, the parameter χ, which presents the rigidity ratio of the rotational spring, the ratio of rigid zone(λ_1), and looseness of screw(λ_2) are 8, 0.03 and 0.02 in value respectively.

5.1 Grid Dome

<Fig. 11> is the analytical results under the first case for grid dome. Where the symbol represents yielding springs assumed by <Fig. 1>. And the solid and dotted line indicates distribution of axial force. In case of the more strong color line, axial force is larger. Where N_{el} and $N_{\max}$ are axial force of each element and maximum axial force respectively. The analytic result is shown in <Fig. 11(a)>, when pipe and connector are $\Phi-139.8\times4.0$ and $\Phi-35$. As a result, the elasto-plastic buckling load is $8.04\,t$ and spring is yielded at part of maximum axial force, namely at the vertex of hexagonal plan. The maximum displacements are appeared at the node of number 4, 14, 24, 34, 44 and 54 shown in <Fig. 11(a)>. The curves in Fig. 10 indicate the condition that axial force and bending moment of spring reach yielding.

<Fig. 11(b)> shows the analytic result when diameters of connectors yielded are increased to 40mm. The elasto-plastic buckling load is $9.89\,t$, which is increased to about 20% as compared with the result of <Fig. 11(a)>. Also, the part of maximum axial force is moved into the dome as shown in <Fig. 11(b)>. <Fig. 11(c)> shows the analytic result when diameters of connectors and pipes yielded are 40mm and $\Phi-165.2\times4.5$ respectively. The elasto-plastic buckling load is increased

to about 24% compared with analytic result of Fig. 11(a). And the maximum displacements appeared at the node of number 9, 19, 29, 39, 49, 49, and 59.

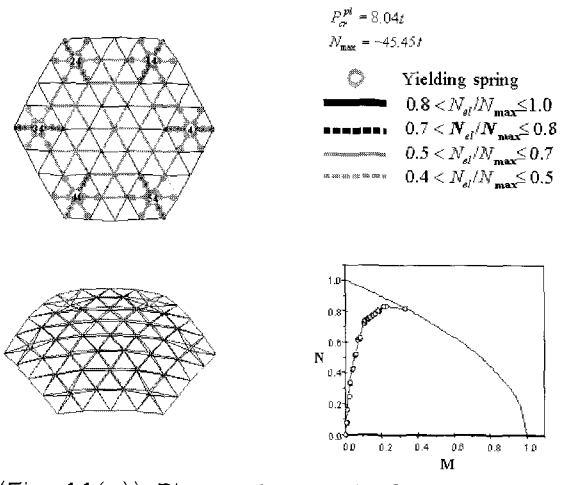

〈Fig. 11(a)〉 Pipe Φ139.8×4.0, Connector Φ35

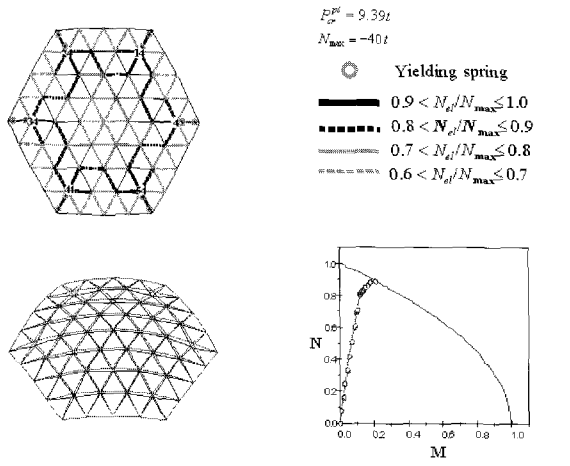

〈Fig. 11(b)〉 Pipe Φ139.8×4.0, Connector Φ40

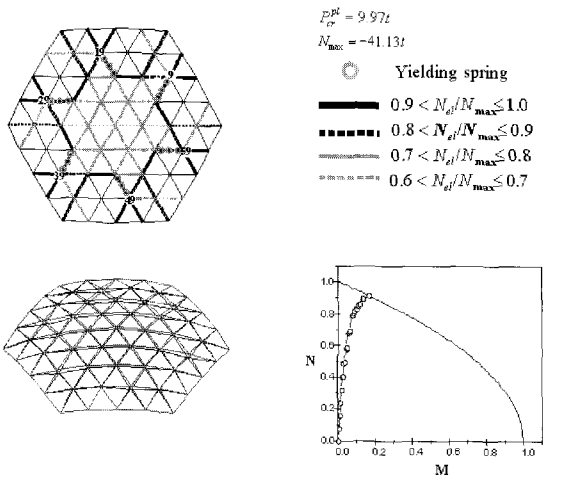

〈Fig. 11(c)〉 Pipe Φ165.2×4.0, Connector Φ40

5.2 Lamella Network Dome

The analytic result is shown in <Fig. 12 (a)>, when dimensions of pipe and connector are $\Phi-139.8\times4.0$ and $\Phi-35$. As a result, the elasto-plastic buckling load is 7.34 t and spring is yielded at part of maximum axial force. But maximum axial force showed unlike Grid Dome from domes center part. The maximum displacements are appeared at the node of number 10, 12, 14, 16, 18, 20, 22 and 24 shown in <Fig. 12(a)>.

<Fig. 12(b)> shows the analytic result when diameters of connectors yielded are increased to 40mm. The elasto-plastic buckling load is 7.55 t. <Fig. 12(c)> shows the analytic result when diame-

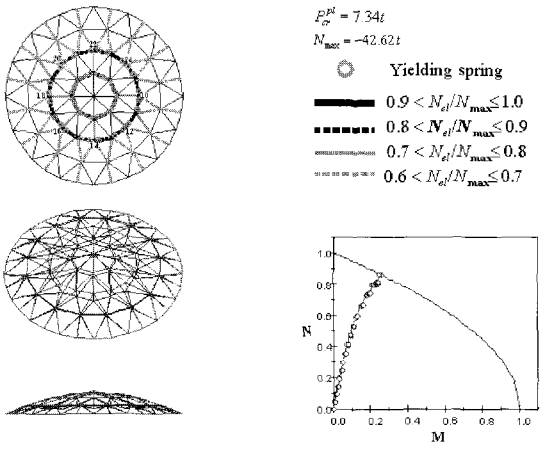

Fig. 12(a) Pipe Φ139.8×4.0, Connector Φ35

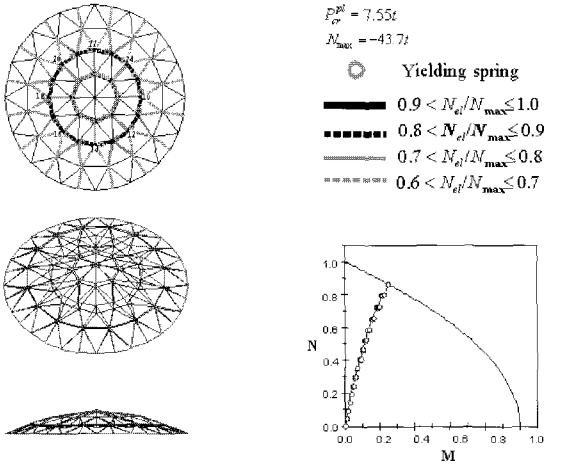

〈Fig. 12(b)〉 Pipe Φ139.8×4.0, Connector Φ40

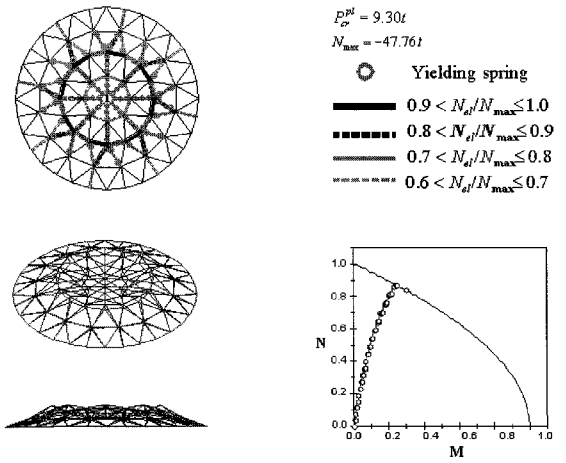

〈Fig. 12(c)〉 Pipe Φ165.2×4.0, Connector Φ40

ters of connectors and pipes yielded are 40mm and $\Phi-165.2\times4.5$ respectively. The elasto-plastic buckling load is increased by about 26% compared with analytic result of <Fig. 12(a)>. The yielding spring appeared on the whole part around the domes crown.

5.3 Geodesic Dome

<Fig. 13> shows the analytic result with Geo-0desic Dome. This figures show that Geodesic Dome is not affected largely by the variation of pipe and connector diameter rather than the Lamella Network and Grid Dome.

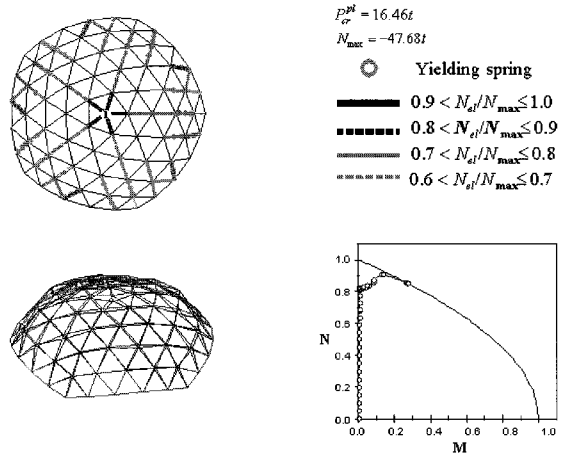

〈Fig. 13(a)〉 Pipe Φ139.8×4.0, Connector Φ35

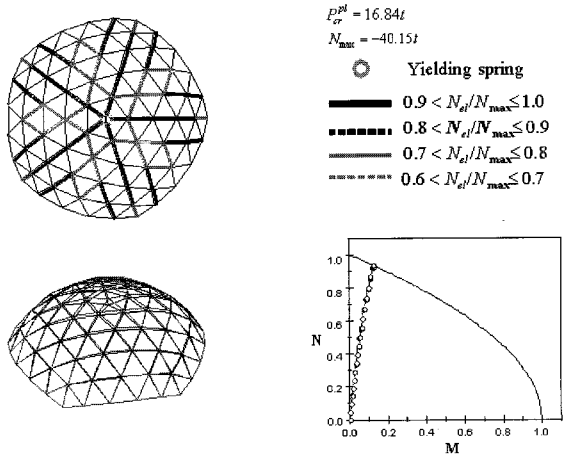

〈Fig. 13(b)〉 Pipe Φ139.8×4.0, Connector Φ40

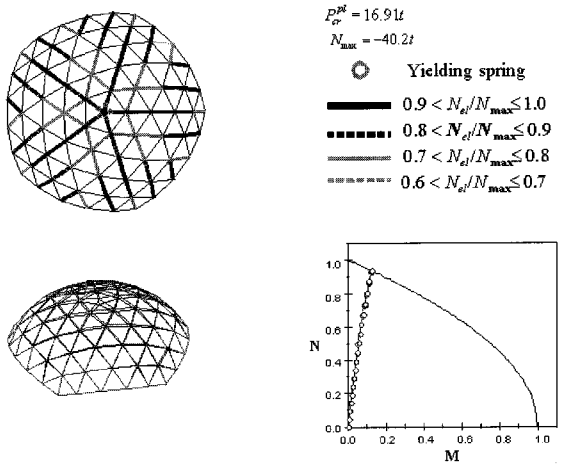

〈Fig. 13(c)〉 Pipe Φ165.2×4.0, Connector Φ40

6. CONCLUSIONS

The characteristics of the connector having an influence on the elasto-plastic buckling load of ball-jointed single layer latticed dome, which is mostly used for the spatial structure recently, are presented in this paper. Analytic results for this study are summarized as follows.

(1) In case of pin support, the elasto-plastic buckling load increases to about 20~40% according as the diameters of the connector are increased. However, the diameters of the connector have not so much effects on the elasto-

plastic buckling load in case of roller support.

(2) Reduction rate of the elasto-plastic bucking load is large when the looseness of screw λ_2 is under 0.02 in case of pin support. From this result, the looseness of screw has a prominent effect on initial instability.

(3) As diameter of the connector is increased, the elasto-plastic buckling load is also increased in case of both pin and roller supports.

(4) Results of elasto-plastic analysis through changing the section area of yielding part.

The elastoplastic buckling load is increased to about 20% when the connectors section area of yielding parts are increased. It is verified that Grid Dome of hexagonal symmetric plan with regular member length is influenced by the increment of the connectors diameter. But, in case of Geodesic Dome of pentagonal asymmetric plan with irregular member length, elasto-plastic load is not so much influenced by the variation of connectors diameter.

Reference

1. Ueki, T., Kato, S., Kubodera, I., and Mukaiyama, Y., Study on the Elastic and Elasto-Plastic Buckling Behavior of Single Layered Domes Composed of Members having Axial and Bending Springs at Both Ends, Proc. of the International IASS Symposium, 1991, Vol. 3, pp. 93~100.
2. Suzuki, T., Ogawa, T., Kubodera, I, and Ikarashi, K., Experiment and Elasto-Plastic Buckling Analysis of Ball-jointed Single Layer Reticulated Domes(in Japaness), Transactions of AIJ, 1993, No. 444, pp. 53~62.
3. Ueki, T., Mukaiyama, Y., Shomura, M., and Kato, S., Loading Test and Elasto-Plastic Buckling Analysis of a Single layer Latticed Dome (in Japaness), Transactions of AIJ, 1991, No. 421, pp. 117~128.
4. Takashima, H. and Kato, S., Numerical Simulation of Elastic-Plastic Buckling Behavior of a Reticular Domes, Space Structures, 1993, Vol. 2, pp. 1314~1322.
5. Crisfield, M. A., Non-linear Finite Element Analysis of Solids and Structures John Wiley & Sons Ltd, New York, 1991. Vol. 1, pp. 24~4.